Non-Doped and Unsorted Single-Walled Carbon Nanotubes as Carrier-Selective, Transparent and Conductive Electrode for Perovskite Solar Cells

Takahiro Sakaguchi,[1,†] Il Jeon,[1,†] Takaaki Chiba,[1] Ahmed Shawky,[1,2] Rong Xiang,[1] Shohei Chiashi,[1] Esko I. Kauppinen,[3] Nam-Gyu Park,[4,*] Yutaka Matsuo,[1,5,*] Shigeo Maruyama[1,6,*]

[1] Department of Mechanical Engineering, School of Engineering, The University of Tokyo, 7-3-1 Hongo, Bunkyo-ku, Tokyo 113-8565, Japan

[2] Nanomaterials and Nanotechnology Department, Advanced Materials Division, Central Metallurgical Research and Development Institute (CMRDI), P. O. Box 87, Helwan 11421, Cairo, Egypt

[3] Department of Applied Physics, School of Science, Aalto University 15100, FI-00076 Aalto, Finland

[4] School of Chemical Engineering and Department of Energy Science, Sungkyunkwan University, Suwon 440-746, Korea

[5] Hefei National Laboratory for Physical Sciences at Microscale, University of Science and Technology of China, 96 Jinzhai Road, Hefei, Anhui 230026, China

[6] Energy NanoEngineering Laboratory, National Institute of Advanced Industrial Science and Technology (AIST), 1-2-1 Namiki, Tsukuba 205-8564, Japan

[§] Electronic Supplementary Information (ESI) available: [details of any supplementary information available should be included here]. See DOI: 10.1039/x0xx00000x

[†] These authors contributed equally (T.S. and I.J.).

The authors declare no competing financial interests.

[*] E-mail: npark@skku.edu (N.P.); matsuo@photon.t.u-tokyo.ac.jp (Y.M.); maruyama@photon.t.u-tokyo.ac.jp (S.M.)

Abstract:

Lead halide perovskite solar cells with a structure of glass/FTO/TiO_2/$CH_3NH_3PbI_3$ with single-walled carbon nanotubes (SWNT) as the transparent top electrodes, followed by polymethyl methacrylate (PMMA) over-coating were fabricated. The SWNT-based perovskite solar cells do not require expensive metal electrodes and hole-transporting materials yet produce a decent power conversion efficiency of 11.8%, owing to the densifying effect of SWNTs by PMMA. The resulting devices demonstrate reduced hysteresis, improved stability, and increased power conversion efficiency.

Introduction

Single-walled carbon nanotubes (SWNTs) have been explored by researchers from various fields because of the unique 1D structure and exceptional electrical properties, namely high carrier mobility, mechanical and thermal robustness. [1] However, the interface engineering of SWNTs has not been fully understood when they are incorporated in 3D devices. Here, we discuss the application of SWNT films in Lead halide perovskite solar cells (PSCs) which have emerged recently. PCSs have attracted much attention around the world as the efficient alternative energy harvesting devices.[2] Miyasaka and colleagues demonstrated the first application of perovskite materials in replacement of organic dyes.[3] The research gained momentum when Park and colleagues resolved the instability issue of the perovskite materials in the electrolyte by developing a solid-state submicron perovskite layer.[4] Now, the certified power conversion efficiencies (PCEs) exceed 22%.[5] Despite the high PCEs, the low stability and high fabrication-cost of PSCs still remain as unresolved problems. Lately, SWNT electrodes have been used as an electrode in PSCs to solve aforementioned problems by replacing expensive metal electrodes.[6-9] However, the devices still rely on hole-transporting materials (HTMs), which are also expensive and impose stability limitation.[10,11]

In this work, SWNT-based PSCs where SWNTs are replacing the metal electrodes were fabricated without the use of HTMs. There have been numerous reports claiming that thick SWNTs can function as the HTM, contradicting high purity semiconducting SWNTs.[12,13] It was our prognosis that we could achieve high-performance PSCs without the use of HTMs by employing SWNT as the top electrode. Lead halide perovskite was deposited via the one-step adduct method,[14] followed by SWNTs lamination. The metal- and HTM-free PSCs produced a PCE of 10.0%. Upon drop-casting poly(methyl methacrylate) (PMMA) on top of SWNTs, the PCE

increased to 11.8%. Moreover, the hysteresis was reduced and the stability of the devices was improved significantly. According to our analyses, the application of PMMA-densified SWNT film increased every photovoltaic parameter, namely short-circuit current (J_{SC}), open-circuit voltage (V_{OC}), and fill factor (FF). This was due to the densification of SWNTs by PMMA, which increased the conductivity of SWNT films. PMMA also functioned as an effective encapsulation, improving the stability.

Methodology

Synthesis of SWNT Films

Randomly oriented SWNT networks with high purity and long nanotube bundle length can be synthesized by the aerosol chemical vapor deposition (CVD) method. [15] The floating catalyst aerosol CVD was carried out in a scaled-up reaction tube with a diameter of 150 mm. The catalyst precursor was vaporized by passing ambient temperature CO through a cartridge filled with ferrocene powder. To obtain stable growth of SWNTs, a controlled amount of CO_2 was added to the carbon source (CO). SWNTs were directly collected downstream of the reactor by filtering the flow through a nitrocellulose or silver membrane filter (Millipore Corp., USA; HAWP, 0.45 μm pore diameter). The flow containing ferrocene vapor was then introduced into the high-temperature zone of a ceramic tube reactor through a water-cooled probe and mixed with additional CO. Ferrocene vapor was thermally decomposed in the gas phase of the aerosol CVD reactor at the 880 $^{\circ}$C. The CO gas was supplied at 4 L min $^{-1}$ and decomposed on the iron nanoparticles, resulting in growth of SWNTs. The as-synthesized SWNTs were collected by passing the flow through microporous filters at the downstream of the reactor, while the transparency and sheet resistance were controlled by varying the collection time. The collected SWNT networks were transferred to

a variety of substrates through the dry press-transfer process. The FC-CVD synthesized and dry deposited SWNT networks were of high purity. Furthermore, as the process requires no sonication-based dispersion steps the resulting SWNT network consisted of exceptionally long SWNTs.

Solar Cell Fabrication

Fluorine-doped tin oxide (FTO) (Peccell Technologies, ~10 Ω cm $^{-2}$) were used after sequential cleaning in isopropanol, acetone, and distilled water using an ultrasonic bath (5 min each), followed by annealing at 500 °C. A compact TiO_2 layer on the FTO-coated glass substrates was prepared by spin-coating of titanium diisopropoxide bis(acetylacetonate) solution (0.15 M, in ethanol) at 5,000 rpm for 30s, dried at 125 °C for 5 min, then repeated twice with 0.3 M of titanium diisopropoxide bis(acetylacetonate) solution, finally annealed at 500 °C for 15 min.

The $MAPbI_3$ perovskite layers were fabricated via Lewis base adduct method described by Ahn et al.[14] A 1:1:1 molar ratio mixture of PbI_2 (TCI), MAI (TCI),[4] and dimethyl sulfoxide (DMSO) (Sigma-Aldrich) was dissolved in dimethylformamide (DMF) (Sigma-Aldrich) at 50 wt% without heating. The fully dissolved solution was spin coated onto TiO_2 layer at 4000 rpm for 30 s, with a dropping of 0.1 mL diethyl ether 7.5 s after starting the spin-coating process. The transparent green film, so-called CH_3NH_3I•PbI_2•DMSO adduct film, changed to a dark brown color by heating at 100 °C for 20 min.

SWNT film was applied directly onto the perovskite film using a pair of tweezers. A drop of chlorobenzene was applied to improve the contact between the perovskite film and the SWNT film. The SWNT film was *ca.* 200 nm thick. Three droplets of PMMA, which was prepared by dissolving 1mg of PMMA (Average Mw ~996,000 by GPC crystalline, Aldrich) in 100 mg of

anisole (Aldrich), were applied to densify the SWNT film. This was followed by annealing at 80 °C for the 30s. The thickness of the SWNT film reduced to *ca*. 100 nm due to densification.

Characterizations

J–V characteristics were measured by software-controlled source meter (Keithley 2400) in dark conditions and 1 sun AM 1.5G simulated sunlight irradiation (100 mW/cm^2) using a solar simulator (EMS-35AAA, Ushio Spax Inc.) with Ushio Xe short ark lamp 500, which was calibrated using a silicon diode (BS-520BK, Bunkokeiki). Shimadzu UV-3150 was used for the UV-vis-NIR measurement. Integrated photoconversion efficiency (IPCE) system consisted of an MLS-1510 monochromator to scan the UV-vis spectrum. A source measurement unit was used to record the current at each specific wavelength. Valence band information and Fermi levels were measured by Riken Keiki photoelectron yield spectroscopy (PYS) PYS-A AC-2 and Kelvin probe S spectroscopy in the air (ESA), respectively. They were calibrated by Au before the measurement. Solartron SI1287 Electrochemical Interface and Solartron 1255B Frequency Response Analyzer were used for the Impedance Measurement. Photoluminescence was measured using JASCO FP6500 spectrophotometer; at room temperature (298 K) in a 1 x 1 cm glass substrate. An excitation wavelength of 500 nm was used.

Results and discussion

Recently, SWNT has been regarded as promising electrodes for in PSCs since earth-abundance, easy synthesis, and direct roll-to-roll expected processability. [16] High quality and directly transferrable SWNT films have been developed by Kauppinen and colleagues. [15] The randomly oriented SWNT networks with high purity were synthesized using the aerosol chemical

vapor deposition (CVD). Floating catalyst aerosol CVD was performed in a tube with a diameter of 150 mm. As the process did not require dispersion step, the resulting SWNT network contained long SWNTs. The SWNT films were easily peeled off from a nitrocellulose film and transferred onto the perovskite layer of PSCs (glass/FTO/TiO_2/$CH_3NH_3PbI_3$) using a pair of tweezers. [17] A few drops of chlorobenzene were added to enhance the interface adhesion between the SWNT film and the perovskite layer. In the case of PMMA-applied CNT-laminated PSCs, we applied the solution of PMMA onto the SWNT film instead of chlorobenze.

According to the photovoltaic measurements in Figure 1, SWNT-applied metal-free PSCs produced a PCE of 10.0% even in the absence of HTMs. This was due to the fact that both the perovskite layer ($CH_3NH_3PbI_3$) and SWNTs can partially function as the HTM. [12,13,18] A recent study by Blackburn and colleagues proved that an interface dipole is formed through the selective charge transfer from methylammonium ion to SWNT, leading to the band alignment. [19] A simple over-coating of SWNT film with a solution of PMMA increased the PCE by approximately 2%. This improvement was due to the increases in all three photovoltaic parameters, V_{OC}, J_{SC}, and FF (Table 1). From the photovoltaic data and current-voltage ($J-V$) curves, we observed that the difference between forward and reverse $J-V$ curves was much reduced (Figure 1). This indicates that the application of PMMA reduced hysteresis. Cross-sectional scanning electron microscopy (SEM) images in Figure 2 show the interface between SWNT film and the perovskite layer. Before the application of chlorobenzene, some parts of the SWNT film do not make full contact with the perovskite layer (Figure 2b). After the application of chlorobenzene, magnified SEM images show that the SWNT film makes full contact with the perovskite layer. From Figure 2d, we can see that the addition of PMMA densifies the SWNTs. Polymeric gel-like PMMA seems to have percolated into the network of SWNTs, filling the air gaps and reducing the thickness of the SWNT film.

From the $J-V$ curves in Figure 1a, we can see that the application of PMMA reduced hysteresis. The reduction in hysteresis can also be explained by the decreased trapped charge in the SWNT film. According to the study conducted by Choi and colleagues, [20] hysteresis is caused by trapped charge at the interface of perovskite layer and can be reduced by effective charge extraction. Our hypothesis is that the densification of SWNTs by PMMA can extract trapped charge more effectively through the better adhesion between SWNTs and perovskite layer (seen by arrows in Figs 2c, 2d).

The role of PMMA was not limited to densifying the SWNT network, it also encapsulated the devices against atmospheric moisture effectively. Although SWNT has the hydrophobic nature, our water vapor transmittance rate (WVTR) measurements show that the SWNT film alone was not enough to block moisture and that the application of PMMA greatly improved the barrier ability of SWNTs (Figure S1). Indeed, the stability tests in ambient conditions and under 1 sun showed that the PMMA applied-devices were much more stable compared to the PSCs without PMMA as displayed in Figure 3. In particular, the stability test under one sun indicates degradation induced by trapped charges seen in Figure 3b. The fact that the PMMA-applied devices lasted longer indicates that PMMA-densified SWNT film reduced trapped charges, which triggers light-induced degradation.

The improvement in J_{SC} and FF were investigated using various analyses. The UV-vis transmittance spectra in Figure S2b showed no difference. However, the IPCE spectra in Figure S2a shows that there is an increase of the integrated J_{SC} of *ca.* 2.78 $mAcm^{-2}$, indicating a better contact between perovskite and SWNT with PMMA. This reveals that the PMMA had no optical effect because the sunlight was shone from the FTO side, and the increase in J_{SC} was not influenced by absorption but solely by the improved contact. [21] To investigate charge extraction after the

PMMA application, photoluminescence (PL) and impedance measurement were conducted. From the PL measurement data in Figure 4a, the suppression of the lead halide perovskite film PL spectrum is patently observable after the deposition of SWNT compared to PMMA-densified SWNTs. While this confirms efficient charge extraction, the difference in charge extraction after the PMMA application was difficult to observe even after magnification of the intensity by fifty-fold. In general, a Nyquist plot is based on an equivalent circuit of PSCs, consisting of a series resistance (R_s, starting point of the first semicircle of the Nyquist plot), electron transport resistance at the counter electrode (R_{ct}, first semi-circle in the Nyquist plot), and recombination resistance (R_{rec} second semicircle in the Nyquist plot) as shown in Figure S3.[22] Accurate comparisons of R_{ce} and R_{rec} can be made by reading impedance graphs over different potentials (Figure 4b-c). It is well known that R_s and R_{ct} are parts of the total series resistance of PSCs. [23] Looking at the starting position of the curves in the Nyquist plot in Figure S3, PMMA-applied PSCs have a similar R_s. However, PMMA-applied PSCs showed a lower R_{ct} compared to the devices without the application of PMMA, with no significant change in R_{rec}. This indicates that it was the densification of SWNT electrode by PMMA that led to more efficient charge extraction with reduced hysteresis and increased FF. Because the increase in both J_{SC} and FF can be caused by a doping effect of PMMA on SWNT, as previously been reported by several groups, [24–30] we used four-probe measurement PYS to confirm the effect. For the four-probe measurement, we pasted indium at the four corners of a pristine SWNT film and then spin-coated the film with PMMA (Figure S4). There was a sheet resistance change before and after the PMMA deposition on a pristine SWNT film. We observed a decrease in sheet resistance by approximately 6 Ωcm^{-1}. According to the PYS measurement result in Figure S5, SWNT film has a Fermi level of around 5.0 eV. After PMMA was applied to the SWNT film, it became impossible to detect the Fermi

level. This was due to the PMMA coverage at the surface insulating electron transfer, making the Fermi level undetectable by PYS. We carried out vis-NIR (near infra-red) absorption spectroscopy on SWNT films with and without PMMA. We found that the Van Hove peaks get weakened upon PMMA application, followed by thermal annealing (Figure S6). This indicates that there might be a possible doping effect of PMMA on SWNTs, yet it is not conclusive at this stage.

Conclusion

In conclusion, we demonstrated decent performance SWNT-based PSCs without expensive metal electrodes and HTMs. By overcoating with PMMA, the SWNT film was densified which led to the PCE increase, reduction in hysteresis, and stability improvement in air. We are confident that the demonstration of metal- and HTM-free PSCs and the discovery of SWNT densification by PMMA will accelerate carbon-based solar cell research and commercialization.

Electronic Supplementary Information (ESI)

The ESI contains WVTR test results, IPCE and UV-Vis spectroscopy, Nyquist plot of impedance measurement, four-probe measurement, and photoelectron yield spectroscopy.

Acknowledgments

We gratefully acknowledge the Research and Education Consortium for Innovation of Advanced Integrated Science by Japan Science and Technology (JST) and Japan Society for the Promotion of Science (JSPS) KAKENHI Grant Numbers (JP25107002, JP15H05760, and 17H06609), the CREST project, and IRENA Project by JST-EC DG RTD, Strategic International Collaborative Research Program, SICORP. Part of this work is based on results obtained from a project commissioned by the New Energy and Industrial Technology Development Organization (NEDO). N.-G.P. acknowledges financial support from the National Research Foundation of Korea (NRF) grant funded by the Ministry of Science, ICT & Future Planning (MSIP) of Korea under contract No. NRF-2012M3A6A7054861 (Global Frontier R&D Program on Centre for Multiscale Energy System).

References

1. A. Jorio, G. Dresselhaus, M. S. Dresselhaus, Carbon Nanotubes - Advanced Topics in the Synthesis, Structure, Properties, and Applications-, Springer-Verlag, Berlin (2008).
2. M. A. Green, A. Ho-Baillie and H. J. Snaith, The emergence of perovskite solar cells, *Nat. Photonics* **8**, 506 (2014).
3. A. Kojima, K. Teshima, Y. Shirai and T. Miyasaka, Organometal Halide Perovskites as Visible-Light Sensitizers for Photovoltaic Cells, *J. Am. Chem. Soc.* **131**, 6050 (2009).
4. H.-S. Kim, C.-R. Lee, J.-H. Im, K.-B. Lee, T. Moehl, A. Marchioro, S.-J. Moon, R. Humphry-Baker, J.-H. Yum, J. E. Moser, M. Grätzel, and N.-G. Park, Lead Iodide Perovskite Sensitized All-Solid-State Submicron Thin Film Mesoscopic Solar Cell with Efficiency Exceeding 9%, *Sci. Rep.* **2**, 591 (2012).

5. W. S. Yang, B. -W. Park, E. H. Jung, N. J. Jeon, Y. C. Kim, D. U. Lee, S. S. Shin, J. Seo, E. K. Kim, J. H. Noh, S. I. Seok, Iodide management in formamidinium-lead-halide-based perovskite layers for efficient solar cells, *Science* **356**, 1376 (2017).
6. I. Jeon, T. Chiba, C. Delacou, Y. Guo, A. Kaskela, O. Reynaud, E. I. Kauppinen, S. Maruyama, and Y. Matsuo, Single-Walled Carbon Nanotube Film as Electrode in Indium-Free Planar Heterojunction Perovskite Solar Cells: Investigation of Electron-Blocking Layers and Dopants, *Nano Lett.* **15**, 6665 (2015).
7. N. Ahn, I. Jeon, J. Yoon, E. I. Kauppinen, Y. Matsuo, S. Maruyama, M. Choi, Carbon-sandwiched perovskite solar cell, *J. Mater. Chem. A* **6**, 1382 (2018).
8. Z. Li, S. A. Kulkarni, P. P. Boix, E. Shi, A. Cao, K. Fu, S. K. Batabyal, J. Zhang, Q. Xiong, L. H. Wong, N. Mathews and S. G. Mhaisalkar, Laminated Carbon Nanotube Networks for Metal Electrode-Free Efficient Perovskite Solar Cells, *ACS Nano* **8**, 6797 (2014).
9. K. Aitola, K. Sveinbjörnsson, J.-P. Correa-Baena, A. Kaskela, A. Abate, Y. Tian, E. M. J. Johansson, M. Grätzel, E. I. Kauppinen, A. Hagfeldt and G. Boschloo, Carbon nanotube-based hybrid hole-transporting material and selective contact for high efficiency perovskite solar cells, *Energy Environ. Sci.* **9**, 461 (2016).
10. H. Chen and S. Yang, Carbon-Based Perovskite Solar Cells without Hole Transport Materials: The Front Runner to the Market?, *Adv. Mater.* **29**, 1603994 (2017).
11. Z. Wu, T. Song and B. Sun, Carbon-Based Materials Used for Perovskite Solar Cells, *Chem. Nano Mat.* **3**, 75 (2017).
12. I. Jeon, Y. Matsuo and S. Maruyama, Single-Walled Carbon Nanotubes in Solar Cells, *Top. Curr. Chem.* **376**, 1 (2018).P. Schulz, A. -M. Dowgiallo, M. Yang, K. Zhu, J. L. Blackburn, J. J. Berry, Charge Transfer Dynamics between Carbon Nanotubes and Hybrid Organic

Metal Halide Perovskite Films, *J. Phys. Chem. Lett.* **7**, 418 (2016).

13. N. Ahn, D.-Y. Son, I.-H. Jang, S. M. Kang, M. Choi and N. Park, Highly Reproducible Perovskite Solar Cells with Average Efficiency of 18.3% and Best Efficiency of 19.7% Fabricated via Lewis Base Adduct of Lead(II) Iodide, *J. Am. Chem. Soc.* **137** 8696 (2015).
14. A. G. Nasibulin, A. Kaskela, K. Mustonen, A. S. Anisimov, V. Ruiz, S. Kivistö, S. Rackauskas, M. Y. Timmermans, M. Pudas, B. Aitchison, M. Kauppinen, D. P. Brown, O. G. Okhotnikov and E. I. Kauppinen, Multifunctional Free-Standing Single-Walled Carbon Nanotube Films, *ACS Nano* **5**, 3214 (2011).I. Jeon, S. Seo, Y. Sato, C. Delacou, A. Anisimov, K. Suenaga, E. I. Kauppinen, S. Maruyama, Y. Matsuo, Perovskite Solar Cells Using Carbon Nanotubes Both as Cathode and as Anode, *J. Phys. Chem. C* **121**, 25743 (2017).
15. I. Jeon, C. Delacou, A. Kaskela, E. I. Kauppinen, S. Maruyama, and Y. Matsuo, Metal-electrode-free Window-like Organic Solar Cells with p-Doped Carbon Nanotube Thin-film Electrodes, *Sci. Rep.* **6**, 31348 (2016).
16. W. A. Laban and L. Etgar, Depleted hole conductor-free lead halide iodide heterojunction solar cells, *Energy Environ. Sci.* **6**, 3249 (2013).
17. I. Jeon, K. Cui, T. Chiba, A. Anisimov, A. G. Nasibulin, E. I. Kauppinen, S. Maruyama, and Y. Matsuo, Direct and Dry Deposited Single-Walled Carbon Nanotube Films Doped with MoO_x as Electron-Blocking Transparent Electrodes for Flexible Organic Solar Cells, *J. Am. Chem. Soc.* **137**, 7982 (2015).
18. N. Ahn, K. Kwak, M. S. Jang, H. Yoon, B. Y. Lee, J. Lee, P. V Pikhitsa, J. Byun and M. Choi, Trapped charge-driven degradation of perovskite solar cells, *Nat. Commun.* **7**, 13422 (2016).

19. X. Gan, R. Lv, H. Zhu, L.-P. Ma, X. Wang, Z. Zhang, Z.-H. Huang, H. Zhu, W. Ren, M. Terrones and F. Kang, Polymer-coated graphene films as anti-reflective transparent electrodes for Schottky junction solar cells, *J. Mater. Chem. A* **4**, 13795 (2016).
20. G. Yue, D. Chen, P. Wang, J. Zhang, Z. Hu and Y. Zhu, Low-temperature prepared carbon electrodes for hole-conductor-free mesoscopic perovskite solar cells, *Electrochim. Acta*, , **218**, 84 (2016).
21. Z. Li, P. P. Boix, G. Xing, K. Fu, S. A. Kulkarni, S. K. Batabyal, W. Xu, A. Cao, T. C. Sum, N. Mathews and L. H. Wong, Carbon nanotubes as an efficient hole collector for high voltage methylammonium lead bromide perovskite solar cells, *Nanoscale* **8**, 6352 (2016).
22. A. Pirkle, J. Chan, A. Venugopal, D. Hinojos, C. W. Magnuson, S. McDonnell, L. Colombo, E. M. Vogel, R. S. Ruoff and R. M. Wallace, The effect of chemical residues on the physical and electrical properties of chemical vapor deposited graphene transferred to SiO_2, *Appl. Phys. Lett.* **99**, 122108 (2011).
23. D. B. Farmer, H.-Y. Chiu, Y.-M. Lin, K. A. Jenkins, F. Xia and P. Avouris, Utilization of a Buffered Dielectric to Achieve High Field-Effect Carrier Mobility in Graphene Transistors, *Nano Lett.* **9**, 4474 (2009).
24. I. Jeon, J. Yoon, N. Ahn, M. Atwa, C. Delacou, A. Anisimov, E. I. Kauppinen, M. Choi, S. Maruyama, Y. Matsuo, Carbon Nanotubes versus Graphene as Flexible Transparent Electrodes in Inverted Perovskite Solar Cells, *J. Phys. Chem. Lett.* **8**, 5395 (2017).
25. G. D. M. R. Dabera, K. D. G. I. Jayawardena, M. R. R. Prabhath, I. Yahya, Y. Y. Tan, N. A. Nismy, H. Shiozawa, M. Sauer, G. Ruiz-Soria, P. Ayala, V. Stolojan, a a D. T.

Adikaari, P. D. Jarowski, T. Pichler, S. R. P. Silva, Hybrid Carbon Nanotube Networks as Efficient Hole Extraction Layers for Organic Photovoltaics, *ACS Nano* **7**, 556 (2013).

26. K. Cui and S. Maruyama, Carbon Nanotube-Silicon Solar Cells: Improving performance for next-generation energy systems, *IEEE Nanotechnol. Mag.* **10**, 34 (2016).
27. R. Li, J. Di, Z. Yong, B. Sun and Q. Li, Polymethylmethacrylate coating on aligned carbon nanotube-silicon solar cells for performance improvement, *J. Mater. Chem. A* **2**, 4140 (2014).
28. J.-H. Im, C.-R. Lee, J.-W. Lee, S.-W. Park and N.-G. Park, 6.5% efficient perovskite quantum-dot-sensitized solar cell, *Nanoscale* **3**, 4088 (2011).

Table 1. Photovoltaic data of SWNT-applied PSCs with and without PMMA under one sun

Structure	Bias	V_{OC} (V)	J_{SC} (mA cm^{-2})	FF	PCE (%)
FTO/TiO_2/$MAPbI_3$/SWNT	Reverse	0.89	22.5	0.50	10.0 (9.50±0.55)
	Forward	0.78	19.6	0.33	5.0 (4.76±1.19)
FTO/TiO_2/$MAPbI_3$/SWNT+ PMMA	Reverse	0.92	23.1	0.56	11.8 (11.3±0.6)
	Forward	0.79	23.0	0.44	8.0 (6.5±1.5)

(AM1.5G illumination, 100 mW cm^{-2})

Figure captions

FIG 1. *J*−*V* curves of (a) a SWNT film-laminated PSC with PMMA and (b) the same SWNT film-laminated PSC without PMMA under AM 1.5G one sun illumination (100 mW/cm^2). (The aperture mask area was 0.1 cm^2 with a scan rate of 200 ms from 1.2 V to -0.2 V. Reverse bias was measured first followed by forward bias).

FIG 2. Cross-sectional SEM pictures of (a) a PSC without HTM and metal electrode, (b) a SWNT film-laminated PSC before chlorobenzene addition, (c) a SWNT film-laminated PSC after chlorobenzene addition, and (d) a SWNT film-laminated PSC after PMMA addition, the white arrows showed the effect of chlorobenzene and PMMA addition of filling gaps and increasing the adhesion between SWNT and perovskite layer.

FIG 3. Stability test results of SWNT film-laminated PSCs with PMMA and without PMMA (a) in ambience (25°C, 13%) over time, and (b) under illumination of one sun. (c) Degradation pictures of SWNT film-laminated PCSs with and without PMMA in ambience over time.

FIG 4. (a) Photoluminescence spectra of a $CH_3NH_3PbI_3$ film, a SWNT film laminated on the $CH_3NH_3PbI_3$ film, and a PMMA-applied SWNT film laminated on the $CH_3NH_3PbI_3$ film (intensity enhanced by fifty-fold). (b,c). Impedance charge transfer measurements and recombination measurements derived from Nyquist plots of SWNT film-laminated PSCs with and without PMMA can be seen in Figure S3.

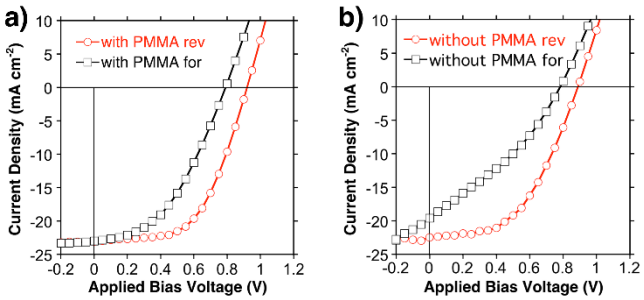
a)
with PMMA rev
with PMMA for
Current Density (mA cm^{-2})
Applied Bias Voltage (V)
b)
without PMMA rev
without PMMA for
Current Density (mA cm^{-2})
Applied Bias Voltage (V)

Fig. 1

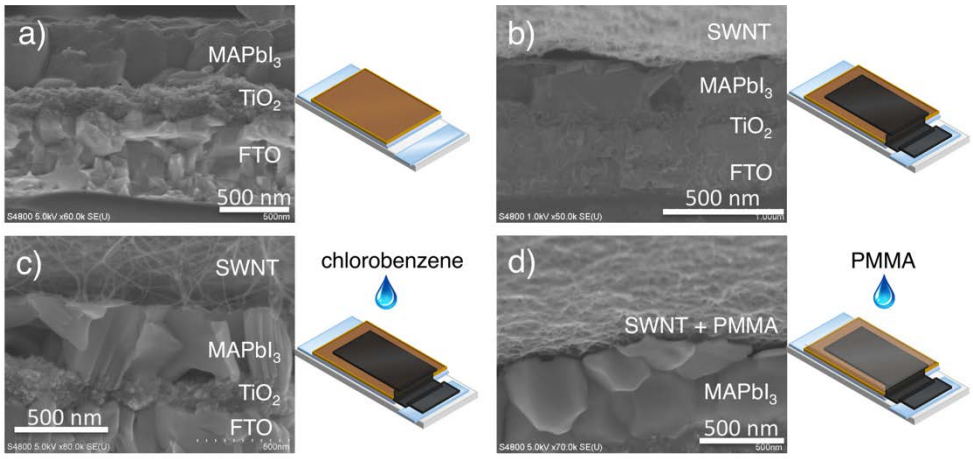
a)
MAPbI$_3$
TiO$_2$
FTO
500 nm
b)
SWNT
MAPbI$_3$
TiO$_2$
FTO
500 nm
c)
SWNT
MAPbI$_3$
TiO$_2$
FTO
500 nm
chlorobenzene
d)
SWNT + PMMA
MAPbI$_3$
500 nm
PMMA

Fig. 2

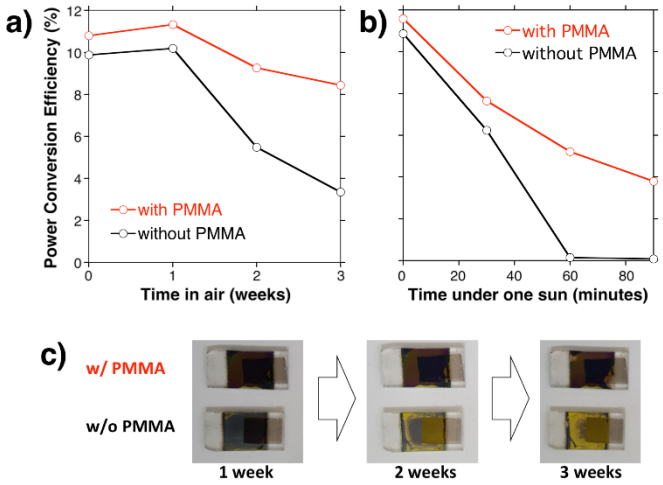
a)
Power Conversion Efficiency (%)
Time in air (weeks)
with PMMA
without PMMA
b)
Time under one sun (minutes)
with PMMA
without PMMA
c)
w/ PMMA
w/o PMMA
1 week
2 weeks
3 weeks

Fig. 3

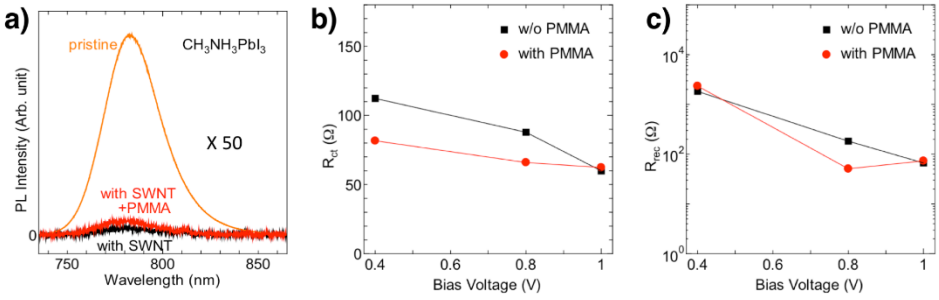
a)
PL Intensity (Arb. unit)
pristine
CH3NH3PbI3
X 50
with SWNT +PMMA
with SWNT
Wavelength (nm)
b)
w/o PMMA
with PMMA
Rct (Ω)
Bias Voltage (V)
c)
w/o PMMA
with PMMA
Rrec (Ω)
Bias Voltage (V)

Fig. 4